Dentin and Enamel Phenotype in Fabry Mice

M. Goldberg[a], D. Septier[a], A. Limaye[b], T. Sreenath[b], A.B. Kulkarni[b]

[a] *Faculté de Chirurgie Dentaire, Université Paris René Descartes, Montrouge, France*
[b] *Functional Genomics Section, Craniofacial Developmental Biology and Regeneration Branch, NIDCR, NIH, Bethesda, Maryland, USA*

Summary: Our aim was to investigate the dental phenotype of α-galactosidase A deficient (AGA-/-) mice - the mutant mice that mimic human Fabry disease. Fabry mice were generated by the gene targeting technique. Segments of mandibles of 21-day-old mice were processed after demineralization for transmission electron microscopy. Comparison was carried out with teeth of mice heterozygous for α-galactosidase A deletion, AGA +/-, (HT). In addition, undemineralized sections of mandibles from one-, six- and 18-month-old mice were observed with a scanning electron microscope. Electron-dense lysosomes containing myelin-like structures loaded the odontoblasts, whereas lipid-like structures were mostly present in intercellular spaces in the enamel organ. The diameter of collagen fibrils in the proximal and distal predentin was identical in the two groups. Metadentin was porous but not enlarged in the Fabry mice. Pericellular collagen fibrils filled the lumen of dentin tubules. Bubble-like structures were seen in the lingual part of mandibular incisors of six-month-old mice, with an increase in number and size at 18 months, suggesting that asymmetric differences exist in the Fabry mice in response to mechanical loading. Although the forming enamel of the Fabry mice displayed porosities containing cell membrane remnants, no defect was detectable in mature enamel. The phenotype differences detected between Fabry and HT mice were discrete and mostly related to odontoblast and dentin. Although the Fabry mice display a lysosomal storage disease, disorders of glycosphingolipid degradation seems to play only a minor role in odontogenesis.

Key words: A-deficient mouse, α-galactosidase, dental abnormalities, Fabry disease, odontogenesis

Oral Biosci Med 2005; 4: 265-271 Submitted for publication 09 November 2004; accepted for publication 16 December 2005

INTRODUCTION

Fabry disease, OMIM 301500, is a rare X-linked lysosomal storage disorder caused by the deficiency of ceramidetrihexosidase, commonly referred to as α-galactosidase A (AGA) (Brady et al, 1967). The gene encoding the enzyme has been localized to the X-chromosomal region, Xq22, and numerous genetic mutations have been reported (Desnick et al, 2001). The enzyme defect causes systemic accumulation of glycosphingolipids with terminal α-D-galactosyl moiety (globotriaosylceramide, digalactosylceramide, blood group B, B1 and P1 glycolipids), and the residues accumulate predominantly within the lysosomes of vascular endothelial cells of various organs including bones (Neufeld, 1991; Kanda et all, 2000; Brady and Schiffmann, 2000; Horiuchi et al, 2002). Major disease manifestations include pain in the extremities, angiokeratomas, corneal dystrophy and vascular disease of the heart, kidney and brain, leading to premature mortality (Desnick et al, 2001; Mohrenschlager et al, 2003). We have earlier reported the high prevalence of oral and dental abnormalities in Fabry patients (Baccaglini et al, 2001). The main dental abnormalities in these patients consisted of malocclusion, diastemas and developmental anomalies.

We have earlier reported generation and characterization of alpha-galactosidase A-deficient mice (Ohshima et al, 1997). Although the mice appear clinically normal at the age of 10 weeks, concentric lamellar inclusions have been observed in the kidney, and lipid analysis revealed a marked accumulation of globotriaosylceramide in the liver and kidneys. These findings indicate similarities between the mutant mice and patients with Fabry disease. The phenotype is also analogous to a chloroquine-induced phospholipidosis (Muller-Hocker et al, 2003). For many years we have investigated the distribution and role of lipids in the dentin and enamel of rats, mice and humans (Goldberg and Boskey, 1996). In the course of these systematic investigations, we have

examined nutritional (zinc, essential fatty acid and vitamin D deficiencies) and pharmacological models (suramin-induced and chloroquine-induced lipidosis). We have also studied animal and human genetic alterations (Zucker rats, Krabbe disease and bone membrane lipodystrophy) (Bloch-Zupan et al, 1994). The information obtained from chemical and morphological studies provide evidence, firstly, for the presence of phospholipids in dentin and enamel, both as membrane or membrane-remnants and extracellular matrix-associated molecules. Secondly, we have shown that experimental or genetic disturbances cause enamel defects and dentin alterations during tooth formation. Altogether, these observations suggest that lipids are implicated in biological and pathological mineralization processes.

In this context, it was interesting to study the phenotype of α-galactosidase A-deficient mice in order to get a better understanding of the alterations produced by this metabolic disorder. To the best of our knowledge, there is no previous report in this domain, and it seemed interesting to investigate the phenotype of the Fabry mice for three reasons. Firstly, a limited repertoire suggests a close relationship between some lipids and collagen fibrillation (LeLous et al, 1982; Pentikainen et al, 1997). Predentin provides a good model to study in vivo interactions between molecules implicated in collagen fibrillation. In this well-organized compartment, the newly secreted collagen fibrils are transported throughout the 15–20μm wide predentin within a period of time comprising between four and six hours. Native collagen fibrils subunits underwent lateral aggregation and increase in diameter from the place where they are secreted to the dentin edge where mineralization occurs (Goldberg et al, 2003). Therefore it was interesting to investigate the effects of the disorder of sphingolipid degradation on collagen fibrillation. Secondly, this may contribute to clarify the relationships between glycosphingolipids and the mineralization processes of dental tissues. Thirdly, it may shed lights on the dental phenotype of the Fabry mice, which are now being utilized for gene therapy approaches to treat this incurable disorder. In the human situation, structural dental alterations, together with mouth dryness - which is a manifestation of the Fabry disease on salivary glands - may favor the development of carious and/or periodontal pathology that interfere with the oral health status of patients.

MATERIALS AND METHODS

Gene targeting and generation of mutant mouse

Fabry mice were generated by gene targeting technique as described (Ohshima et al, 1997). Briefly, murine α-galactosidase A (AGA) gene was cloned earlier from 129SVJ library as described (Ohshima et al, 1995), and the AGA genomic clones were used to construct a gene-targeting vector that disrupts the open reading frame of the AGA gene. A successful gene targeting of the AGA locus in mouse embryonic stem cells was confirmed by Southern blots, and the targeted clones were injected into mouse blastocysts to obtain chimeric mice. The chimeras were mated with wild-type C57BL6A females to generate AGA hemizygus male mice deficient in AGA activity. As reported earlier, these males displayed cumulative accumulation of glycosphyngolipids (Gb3) in the target tissue that mimicked Fabry disease (Ohshima et al, 1997; Ohshima et al, 1995). These mice have been successfully used to develop therapeutic approaches to reverse the Gb3 accumulation (Takenaka et al, 2000; Abe et al, 2000). Fabry mice have been maintained in a specific pathogen-free facility, given food and water ad lib, and cared for as per NIH guidelines.

HISTOLOGICAL PROCEDURES

Light microscopy

Six Fabry mice and six heterozygote mice [HT] mice were sacrificed 21 days after birth, and mandibles were prepared for light microscopy. They were anesthetized with a single intraperitoneal injection of Chloral (400mg/kg body weight). The heads were cut with a razor blade and fixed in 4% paraformaldehyde buffered with 0.1M sodium cacodylate buffered at pH 7.2-7.4 for four hours. They were rinsed in the cacodylate solution, then demineralized in 4.13% EDTA. The tissue was dehydrated in graded ethanols and embedded in Paraplast (Oxford Labware, St Louis, MO, USA). Five μm-thick sections were cut, then dewaxed and stained with Masson's trichrome, or hematoxylin-eosin.

Epon-embedded semi-thin sections and transmission electron microscopy

Six other 21 day-old homozygote Fabry mice and six heterozygote (HT) mice were anesthetized. The mandibles were dissected, reduced in size with a razor blade, and sliced transversally into segments containing the molars and the subjacent incisor. They were immersed in a fixative solution containing a 3.75 M glutaraldehyde solution buffered with 0.1M sodium cacodylate, pH 7.2 for one hour at 4°C. They were rinsed and post-fixed with 2% osmium tetroxide in the same buffer for 30 minutes at room temperature. The segments were demineralized with 4.13% EDTA for three weeks to one month. After dehydration in graded ethanols, the segments were embedded in Epon.

Semi-thin sections were stained with toluidine blue. Ultrathin sections were stained with uranyl acetate and lead citrate and examined with a Jeol 100B transmission electron microscope operating at 80kV.

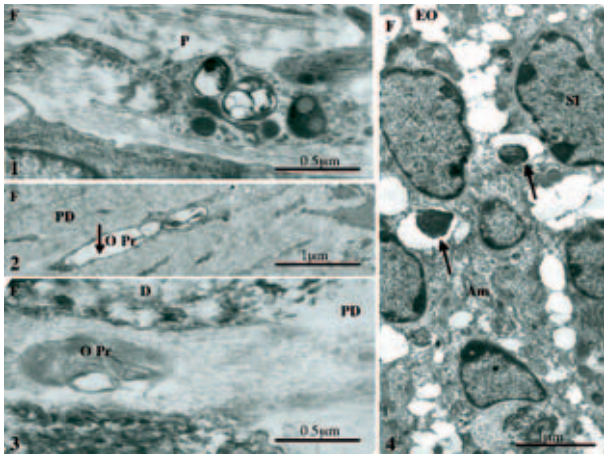

Fig 1 Sub-odontoblastic cell in a Fabry mouse, loaded with lysosome-like structures containing amorphous heterogeneous osmiophilic material. Thin collagen fibrils are seen in the pulp (P). Bar = 0.5µm.
Fig 2 Odontoblast process (O Pr) in predentin (PD) containing large electron-lucent vesicles (arrow). Bar = 1µm.
Fig 3 Odontoblast process (O Pr) inside a dentin tubule. D: dentin, PD: predentin. Bar= 0.5µm.
Fig 4 Enamel organ (EO) in a Fabry mouse (F). Large intercellular osmiophilic structures are seen in the intercellular spaces between cells of the stratum intermedium (SI) and ameloblasts (Am). Bar= 1µm.

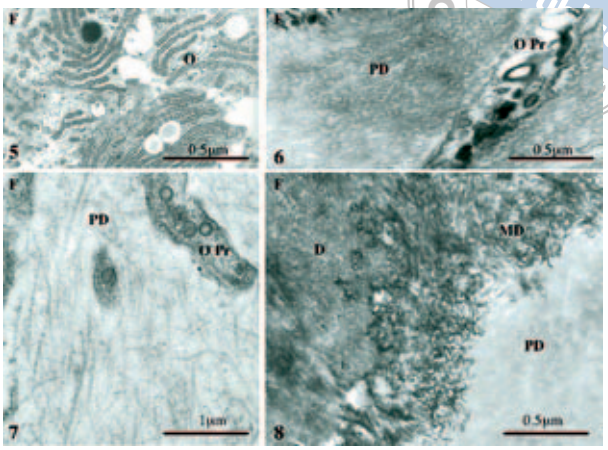

Fig 5 Odontoblasts (O) in a Fabry mouse loaded with lysosome-like structures. Bar= 0.5µm.
Fig 6 Predentin (PD) in a Fabry mouse. The odontoblast process (O Pr) contains numerous structures filled with amorphous electron-dense material. Bar = 0.5µm.
Fig 7 Predentin (PD) containing collagen fibrils. Numerous coated vesicles are seen in the odontoblast process (O Pr). Bar= 1µm.
Fig 8 Predentin (PD), metadentin (MD) and dentin (D) in a Fabry mouse. Metadentin is porous but not enlarged. Bar= 0.5µm.

Calculations of the mean diameter of collagen fibrils were carried out on ultrathin sections from six first mandibular molars per group. Six to nine electron micrographs per tooth, taken systematically in the inner and outer zones, were enlarged at a final magnification x 54.000, and the diameters of 1800-2000 collagen fibrils per group were measured with a glass magnifier equipped with a reticule allowing scoring at a 0.1mm level. Measurements were pooled. The mean value and the standard deviation were calculated. For the fibril density, using the same micrographs, the number of fibrils per μm^2 was calculated from the number of fibrils present in small square areas (2mm x 2mm). Again, this was carried out on the teeth of six mice of each group. Data were analyzed by Student's t test. $P \geq 0.05$ was considered statistically significant.

SCANNING ELECTRON MICROSCOPY

Mandibules were dissected from one-month, six-month and 18-month animals. They were fixed with glutaraldehyde, rinsed, kept in the buffer (sodium cacodylate 0.1M), sectioned transversally with a diamond disc, rinsed and critically point dryed. After sputter coat deposition of a thin film of gold and palladium, sections were observed with the SEM (Jeol 35C) operating at 60kV.

RESULTS

Although the overall appearance of the teeth was close to normality, closer examination with the transmission electron microscope revealed some alterations. Odontoblasts were loaded with electron-dense or electron-lucent lysosome-like structures (Figs 1-3), both in cell bodies (Fig 5) and processes (Fig 6). They appeared either as myelin-like lamellar or dendritic electron-dense inclusions. Such structures were not observed in secretory ameloblasts. However, in the enamel organ of rat incisors, large oval or round electron-dense, large dots containing osmiophilic material, about 0.2µm in diameter, were located in the intercellular spaces (Fig 4). The consequences of the disease were hardly detectable in the proximal predentin (Fig 7). In contrast, metadentin, a 0.5-2.5µm thick layer located at the dentin edge, at the junction between predentin and dentin - a structure also termed mineralization front - was visible despite the fact that a conventional routine method of fixation for electron microscopy was used. In the WT mice, metadentin is usually not visible with conventional aqueous methods of fixation. In the Fabry mice, the band was so porous and wide (2µm) - although within the limits of normality - that it became an individualized structure, distinct from the dentin, which looked like a compact tissue (Fig 8).

The diameter of the collagen fibrils was eventually enlarged between the proximal and distal predentin.

Table 1 Mean diameter of the collagen fibrils in heterozygote mice (HT) and Fabry mice (mean± SD)

Collagen fibril Ø in nm ± SD	HT mice	Fabry Mice
Proximal predentin	19.25 ± 2.45	22.00 ± 3.80
Distal predentin	39.85 ± 3.30	33.50 ± 3.70

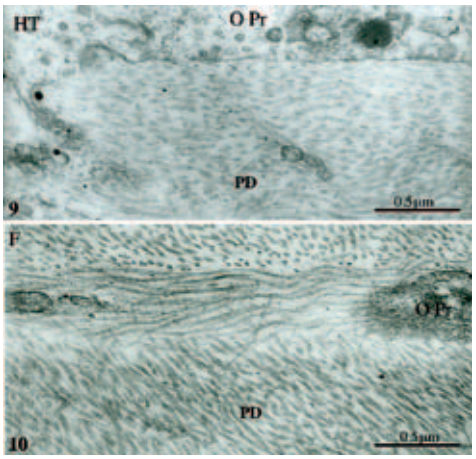

Fig 9 Predentin (PD) and odontoblast process (O Pr) in a wild-type (HT) mouse. Bar= 0.5µm.

Fig 10 Predentin (PD) and odontoblast process (O Pr) in a Fabry mouse. Collagen fibril diameter is apparently the same in homozygote and heterozygote mice, but the fibril density seems to be increased in the Fabry mouse. Numerous collagen fibrils are seen to be longitudinally oriented along the odontoblast process, in a pericellular area. Bar= 0.5µm.

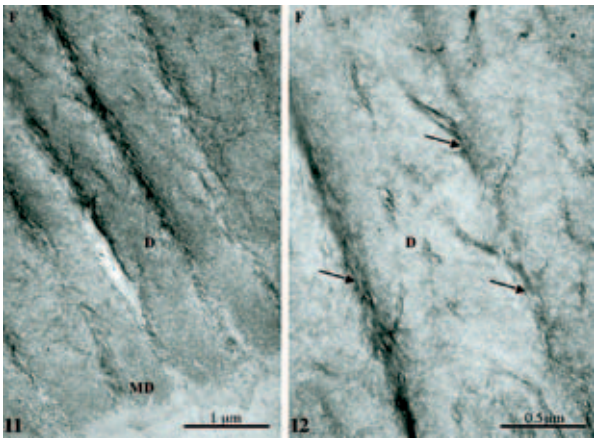

Figs 11 and 12 D= dentin, MD= metadentin. In the Fabry mouse, the lumen of the dentin tubules is filled with collagenous pericellular material (Arrows). Fig 11: bar= 1µm; Fig 12: bar= 0.5µm.

However, no statistically significant difference could be established between the HT and Fabry mice, as shown in Table 1. In the HT mice, collagen fibrils were mostly seen in transverse section, with a few bundles of fibrils cut longitudinally (Fig 9). In the Fabry mice, the fibril density was increased, and bundles of wavy longitudinal fibrils were seen in predentin, in close association with and around the processes (Fig 10). In dentin, in the continuity of what was seen in predentin, a dense and tightly packed pericellular collagen network was also apparent. These collagen fibrils fill a large part, and even the totality of the lumen of the tubules and form dense peritubular structures, never seen in the HT mice. Lateral branching seemed also to benefit from collagen fibrils contribution (Figs 11, 12).

Observation of transverse sections of incisors with the scanning electron microscopy revealed a previously unsuspected age-dependent feature. The first evidence of this alteration was detected in the six-month-old Fabry mice, where a few oval bubbles were seen only in the lingual part of the incisor (Figs 13, 14). The number and size of the bubbles were increased at 18 months (Figs 15, 16). These large porosities seemed to be aligned along the direction of tubules, but were unrelated to these much smaller structures. They were large in the older animals, with 4-8µm in width at six months, and up to 16-20µm at 18 months.

In the forming enamel, minute defects were seen within an amorphous inner enamel layer (Fig 17, 19). At later stages of enamel formation empty spaces related to interrods or to rods were seen. They contained frequently small vesicles, apparently membrane residues (Figs 18, 20). During enamel maturation, beneath a homogeneous outer aprismatic layer (Fig 21), many remnants of ameloblast processes were seen in persisting rod defects, not detected in the HT mice. Large processes remnants were seen to accumulate electron-dense lamellar inclusions (Fig 22).

Examination of etched sections of incisors of HT mice evidenced two thin aprismatic inner and outer borders and the bulk of enamel, which is prismatic (Fig 23). The outer aprismatic layer is subdivided into an inner part, 3µm wide, with parallel rods poorly etched, and an outer 3µm thick layer, with a series of alveoli (Fig 23). In the molar, parallel rows of rods cut longitudinally alternated, whereas another series of rods cut transversally.

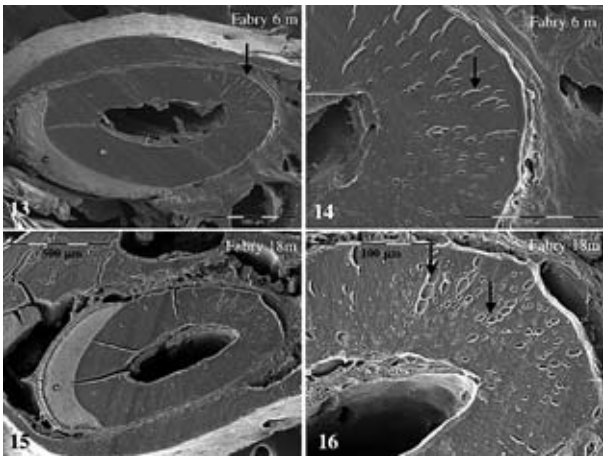

Figs 13 and 14 SEM aspect of an acid-etched section of the mandible of a 6 month-old Fabry mouse. Fissures or bubble-like defects (arrows) are seen in the root-analogue part of the incisor. Fig 13: bar=500μm ; Fig 14: bar=100μm.

Figs 15 and 16 SEM aspect of an acid-etched section of an undemineralized mandible of a 18-month-old Fabry mouse. Aligned bubble-like defects of various size (arrows) are more numerous in the root-analogue part of the incisor of 18-month-old Fabry mouse compared with the 6 month-old mouse. Such defects were not observed in the one-month-old Fabry mouse (data not shown). Fig 15: bar= 500μm; Fig 16: bar=100μm.

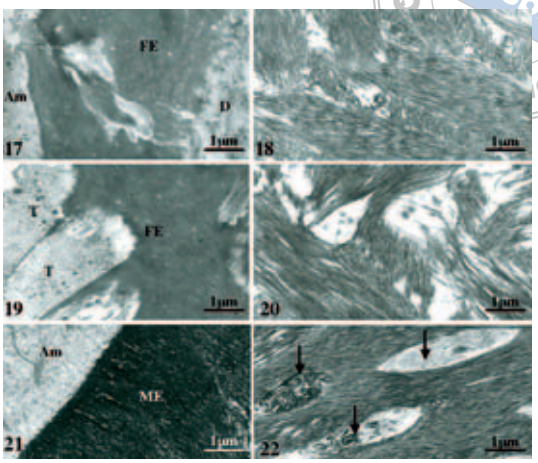

Fig 17 The early forming enamel (FE) in a Fabry mouse appears amorphous, with many electron-lucent minute spaces. Remnants of ameloblast processes (Am) are present inside the forming enamel. D= dentin.

Fig 18 Unfilled minute spaces in the forming enamel of a Fabry mouse.

Fig 19 When the forming enamel (FE) increases in thickness, electron-lucent dots persist. Tomes processes (T) of secretory ameloblasts display normal morphology.

Fig 20 At later stages of enamel formation, large defects are seen to contain small membrane remnants.

Fig 21 Post-secretory ameloblasts (Am) are aligned along the surface of maturing enamel (ME). The enamel outer zone looks normal.

Fig 22 In contrast, in the subsurface zone of maturing enamel, numerous osmiophilic inclusions and membrane remnants (arrows) are seen in spaces that should be filled by enamel rods.

(All figures: bar= 50μm)

Together they form Hunter-Schreger's band. In Fabry and HT mice, the enamel structure was identical. The overall etching pattern was weak at one month, and gradually reinforced at six and 18 months. The outer layer, with a mean thickness of 12.5μm, was not very apparent at one month. At six months the outer amorphous aprismatic border was more visible, with an increased thickness (15-25μm). The thickness was about the same at 18 months (20-25μm in width). This reflected a post-eruptive maturation process (Figs 24-26). No porosity or structural defect could be identified.

DISCUSSION

The present observations firstly provide evidence that, in the Fabry mice, lysosomal storage defects appear inside odontoblasts rather than in the ameloblasts, and therefore influence dentinogenesis rather than amelogenesis. Lysosome-like structures, containing either osmiophilic amorphous material, myelin-like or intracellular accumulation of electron dense dendritic structures gave the cells an appearance reminiscent of what has been reported previously in many lysosomal storage diseases, mainly in lipidosis (Kanda et al, 2000; Lullmann-Rauch, 1979; Iancu, 1992). However, only minor differences were detected between the Fabry mice and HT mice, suggesting that globoside (Gb3, ceramidetrihexoside) accumulation inside lysosomes in odontoblasts does not play a major role in dentinogenesis. It is possible that synthesis ceramides are not secreted, but stored and degraded inside lysosomes. If true, this hypothesis suggests that ceramides play only a minor role in dentin formation. As an alternative possibility, after the normal secretion of the molecule, excesses or partially degraded residual peptides are re-internalized and accumulate inside lysosomes. This second group of events is normally under the control of the ceramidetrihexosidase. As the deficiency impairs the cleavage of the terminal galactose molecule of galactosylglucosylceramide, accumulation of undegraded ceramides occurs inside lysosomes. If the second hypothesis is valid, collagen fibrillation and early post-secretory events have already occurred, and apparently they are not influenced by the enzyme deficiency, providing an overall normal appearance of predentin and dentin. Finally, compensatory mechanisms may also reduce or hide the effects of the deficiency.

Transient alterations were seen in the forming enamel in young mice, but these defects were compensated for in the adult. Although lysosome-like structures accu-

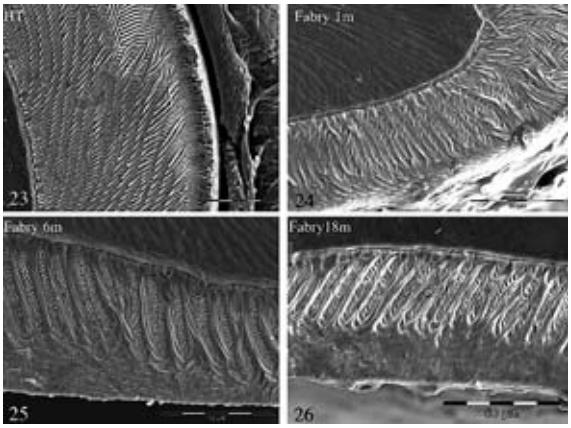

Fig 23 Incisor of heterozygous one-month-old mouse. Mature enamel was etched and observed with the SEM.
Fig 24 One month-old Fabry mouse. Molar. The outer prismatic zone is reduced. Diazones and parazones are seen in the inner enamel.
Fig 25 In the enamel of a six-month-old Fabry mouse's molar, the outer aprismatic zone is thicker.
Fig 26 The outer aprismatic enamel is even thicker and denser in the 18-month-old Fabry mouse.

mulation was not apparent in ameloblasts during enamel secretion and maturation, a delayed degradation of ameloblast Tome's processes was observed, together with extracellular or intercellular accumulation of amorphous osmiophilic structures in the enamel organ. However, this had no apparent consequences on the final enamel structure, which looked very similar in Fabry and HT mice. Consequently, it seems that in the Fabry mouse dentin alterations are observed rather than enamel defects.

Although no striking effect of the disease could be detected in predentin with respect to collagen fibrillogenesis, there is a dental phenotype for the Fabry mice, consisting mostly of an unusual accumulation of collagen fibrils along odontoblast processes in predentin, and inside the lumen of tubules in dentin. Differences between the Fabry mice and the HT mice were also seen at the place where dentin mineralization occurred, i.e. the presence of a large and porous metadentin, suggesting a delayed dentin mineralization (Goldberg and Septier, 1996). Finally, in the lingual part of the incisor, the large dentin defects, which appeared at six months, were increased at 18 months.

Interaction between Type I collagen and lipids was shown in vitro (LeLous et al, 1992). Decorin, associated with the surface of collagen fibrils, links low density lipoproteins (LDL) (Pentikainen et al, 1997). This sheds light on the retention of LDL in collagen-rich areas of atherosclerotic lesions, but finally this phenomenon seems to be unrelated with collagen fibrillation. In contrast, it has been reported that the rate of fibrillogenesis and size of collagen fibrils is diminished by phosphatidylcholine and phosphatidylglycerol vesicles, interacting by peripheral interaction (Martinez del Pozo et al, 1988; 1989). This may be due to electrostatic interference between the positively charged phospholipids molecules and the net positive charge of collagen (McKenzie et al, 1981). Up until now, interaction between Gb3s and collagen fibrillation has not been reported in the literature. In contrast with other lipids, such as acidic phospholipids, Gb3s may have only a small influence on collagen fibrillation.

In predentin and dentin, two distinct groups of collagen fibrils are differently organized. The first group is related to the main bulk of collagen fibrils involved in the interaction with non-collagenous proteins and plays role as a scaffold in the mineralization process occurring in the intertubular dentin. A smaller second group of fibrils is seen only along odontoblast processes in predentin and in the lumen of tubules. These fibrils are never associated with the mineralization process. Even during peritubular dentin formation, this group of collagen fibrils is located exclusively in the lumen of the tubules, along cell processes in species where peritubular dentin is seen, which is not the case in rodents. In the Fabry mice, the presence of this second group is amplified, and from our TEM sections collagen fibrils fill the lumen to the detriment of odontoblast processes. It is not known if there is a chemical difference between the two groups of fibrils. The global dentin matrix composition indicate that 90% is formed mostly by type I collagen, including about 11% Type I collagen in the homotrimer form (Butler, 1984). Type III and V are also present and seem to vary between 1% and 3%, depending of the species and/or culture conditions, as seen in studies that were carried out in vitro. There is also a possibility that other collagen types, such as type VI, are also present in minute amounts, but they have not yet been identified in normal dentin, in contrast with pathological dentin where they have been identified (Waltimo et al, 1994). Symmetrical banded structures (SLS) may be detected both in normal (Warshawsky, 1972) and pathological dentin (Acevedo et al, 1995). However, to the best of our knowledge, the respective distribution of the different types of collagen has not yet been related to any anatomical distribution. During secretion, which occurs mostly in the proximal predentin, lateral aggregation of native fibrils, elongation and transport toward the mineralization front occur (Goldberg et al, 2003; Weinstock and Leblond, 1974).

Post-translational modification of collagen fibrils by lysyl-pyridinoline and pyrrole cross-links also contributes to the stability and to mechanical properties of bone and dentin (Knott and Bailey, 2000). Either different types of collagen are implicated respectively in the two groups of anatomically and functionally distinct dentin collagens, or late cross-linkage may be related to the peri- or intertubular distribution. Whatever may be the answer to this question, the ratio between the two groups is modified in the Fabry mice, and therefore may be under the influence of Gb3.

The dentin phenotype in the Fabry mice also includes the time-dependent development of large fissures in the lingual part of the incisor. These defects were much larger than dentin tubules. The diameter of these oval bubbles was about 4-8μm at six months, and up to 16-20μm in the 18 months old mice. Around twice as many defects were scored for a given arbitrary surface in the 18 months old mice compared with the six months old mice. Such defects were never seen in the Wild-Type mice. They may be the results either of Gb3 accumulation in dentin, which may be lost during the preparation of the samples for SEM. As an alternative explanation, there is a possibility that mechanical pressures are unequally distributed in the mandibular incisor. It may be assumed that the maximal stress is located in the lingual root-analogue part of the incisor, where the dentin covered by a thin cementum is interacting with the alveolar bone through a periodontal ligament (Beertsen and Niehof, 1986). This is not the case for the labial crown-analogue part of the incisor, covered by an enamel organ without any fibrous structural connection with the surrounding bony crypt, and therefore less, or not at all, implicated in the dissipation of stress forces. The two hypotheses might well combine. Although such defects were not seen in molars, in the incisors unequally distributed mineralization defects due to Gb3 accumulation in dentin may contribute to the Fabry mice dental phenotype.

REFERENCES

Abe A, Gregory S, Lee L, Killen PD, Brady RO, Kulkarni A, et al. Reduction of globotriaosylceramide in Fabry disease mice by substrate deprivation. J Clin Invest 2000;105:1563-1571.

Acevedo AC, Chardin H, Septier D, Staub JF, Goldberg M. Effects of thyro-parathyroid ectomy and parathyroidectomy upon dentinogenesis: part II: electron microscopy. Connect Tissue Res 1995;32:269-274.

Baccaglini L, Schiffmann R, Brennan MT, Lancaster HE Jr, Kulkarni AB, Brahim JS. Oral and craniofacial findings in Fabry's disease: a report of 13 patients. Oral Surg Oral Med Oral Pathol Oral Radiol Endod 2001;92:415-419.

Beertsen W, Niehof A. Root-analogue versus crown-analogue dentin: a radioautographic and ultrastructural investigation of the mouse incisor. Anat Rec 1986;215:106-118.

Bloch-Zupan A, Lécolle S, Goldberg M. Galactosylceramidase lipidosis (Krabbe's disease) and deciduous dental tissues. A case report. J Submicrosc Cytol Pathol 1994;26:425-435.

Brady RO, Gal AE, Bradley RM, Martensson E, Warshaw AL, Laster L. Enzymatic defect in Fabry's disease. Ceramidetrihexosidase deficiency. N Engl J Med 1967;276:1163-1167.

Brady RO, Schiffmann R. Clinical features of and recent advances in therapy for Fabry disease. JAMA 2000;284:2771-2775.

Butler WT. Dentin collagen: chemical structure and role in mineralization. In: Linde A (ed) Dentin and Dentinogenesis. Boca Raton, Fla: CRC Press, 1984;37-53.

Desnick, RJ, Ioannou, YA, Eng, CM. Alpha-galactosidase A deficiency: Fabry disease. In: Scriver CR, Beaudet AL, Sly WS, Valle, D (eds). The Metabolic and Molecular Bases of Inherited Disease. New York: McGraw Hill, 2001;3733-3810.

Goldberg M, Boskey AL (1996) Lipids and biomineralizations. Progr Histochem Cytochem 1996;312,1-189.

Goldberg M, Rapoport O, Septier D, Palmier K, Hall R, Embery G, et al. Proteoglycans in predentin: the last 15 micrometers before mineralization. Connect Tissue Res 2003;44:184-188.

Goldberg M, Septier D. A comparative study of the transition between predentin and dentin, using various preparative procedures in the rat. Eur J Oral Sci 1996;104:269-277.

Horiuchi H, Saito N, Kobayashi S, Ota H, Taketomi T, Takoaka K. Avascular necrosis of the femoral head in a patient with Fabry's disease - Identification of ceramide trihexoside in the bone by delayed-extraction matrix-assisted laser desorption ionization-time-of-flight mass spectrometry. Arthritis Rheumatism 2002;46:1922-1925.

Iancu TC. The ultrastructural spectrum of lysosomal storage diseases. Ultrastructural Pathology 1992;16:231-244.

Kanda A, Nakao S, Tsuyama S, Murata F, Kanzaki T.. Fabry disease: ultrastructural lectin histochemical analyses of lysosomal deposits. Wirchows Arch 2000;436:36-42.

Knott L, Bailey AJ. Collagen cross-links in mineralized tissues: a role for the pyrrole cross-link. In: Goldberg M, Boskey A, Robinson C (eds) Chemistry and Biology of Mineralized Tissues. Rosemont, Ill: American Academy of Orthopaedic Surgeons, 2000;125-128.

LeLous M, Boudin D, Salmon S, Polonovski J. The affinity of type I collagen for lipid in vitro. Biochim Biophys Acta 1982;708:26-32.

Lüllmann-Rauch R. Drug-induced lysosomal storage disorders. In: Dingle JT, Jacqueds PJ, Shaw IH (eds). Lysosomes in Applied Biology and Therapeutics. Amsterdam: North Holland, 1979;6,49-130.

Martinez del Pozo A, Onaderra M, Laynez J, Gavilanes JG. Interaction of Type I collagen with phosphatidylcholine vesicles. Collagen Rel Res 1988;8:133-144.

Martinez del Pozo A, Onaderra M, Laynez J, Gavilanes JG. (1989) Interaction of Type I collagen with phospholipid vesicles. Matrix 1989;9:405-410.

McKenzie JC, Belton JC, Klein RM. The effects of dipalmitoyl phosphatidylcholine on the precipitation of native fibrils and segment-long-spacing aggregates from collagen solution. J Supramolec Struct 1981;15:219-234.

Mohrenschlager M, Braun-Falco M, Ring J, Abeck D. Fabry disease: recognition and management of cutaneous manifestations. Am J Clin Dermatol 2003;4:189-196.

Muller-Hocker J, Schmid H, Weiss M, Dendorfer U, Braun GS. Chloroquine-induced phospholipidosis of the kidney mimicking Fabry disease: case report and review of the literature. Hum Pathol 2003;34:285-289.

Neufeld EF. Lysosomal storage diseases. Annu Rev Biochem 1991;60:257-280.

Ohshima T, Murray GJ, Swaim WD, Longenecker G, Quirk JM, Cardarelli CO, et al. Alpha-Galactosidase A deficient mice: a model of Fabry disease. Proc Natl Acad Sci USA 1997;18:2540-2544.

Ohshima T, Murray GJ, Nagle JW, Quirk JM, Kraus MH, Barton NW, et al. Structural organization and expression of the mouse gene encoding alpha-galactosidase A. Gene 1995;166:277-280.

Pentikäinen MO, Öörni K, Lassila R, Kovanen PT. The proteoglycan decorin links Low Density Lipoproteins with collagen type I. J Biol Chem 1997;272:7633-7638.

Takenaka T, Murray GJ, Qin G, Quirk JM, Ohshima T, Qasba P, et al. Long-term enzyme correction and lipid reduction in multiple organs of primary and secondary transplanted Fabry mice receiving transduced bone marrow cells. Proc Natl Acad Sci USA 2000;97:7515-7520.

Waltimo J, Risteli L, Risteli J, Lukinmaa P-L. Altered collagen expression in human dentin: increased reactivity of Type III and presence of Type VI in Dentinogenesis Imperfecta, as revealed by immunoelectron microscopy. J Histochem Cytochem 1994;42:1593-1601.

Warshawsky H. The presence of atypical collagen fibrils in EDTA decalcified predentine and dentine of rat incisors. Archs Oral Biol 1972;17:218-229.

Weinstock M, Leblond CP. Synthesis, migration and release of precursor collagen by odontoblasts as visualized by radioautography after 3H-proline administration. J Biol Cell 1974;60:92-127.

Reprint requests:
Dr M. Goldberg
Faculté de Chirurgie Dentaire, Université René Descartes,
1, rue Maurice Arnoux, 92120 Montrouge, France
Tel: 33 1 58 07 68 08, Fax: 33 1 58 07 68 06
E-mail: mgoldod@aol.com